

AUTOMATIC PRECISE GEOMETRIC CORRECTION FOR HJ-CCD IMAGERY

Tian Ye ^{a,b,*}, Li Haitao ^a, Han Yanshun ^a, Gu Haiyan ^a

^a Institute of Photogrammetry and Remote Sensing, Chinese Academy of Surveying and Mapping, Beijing 100039, P.R. China

^b Institute of Surveying and Geography Science, Liaoning University of Engineering and Technology, Fuxin 123000, P.R. China - tianye.zx@163.com

KEY WORDS: HuanJing(HJ)-CCD imagery, Precise geometric correction, Image Control Point (ICP) database, Automatic image matching, Scale Invariant Feature Transform (SIFT) algorithm, Template matching method, polynomial correction with tiny facet

ABSTRACT:

Since HuanJing(HJ)-satellite has been sent successfully in September 6, 2008, in china, productions of precise geometric correction are imminently needed. Moreover, the demand for rapid processing of remote sensing data for disaster is increasing. Aiming at the characteristics of HJ-CCD imagery, a precise geometric correction technology workflow has been designed, which is a very meaningful work. It mainly includes three parts: image control point (ICP) database construction, automatic image matching and geometric correction model. SIFT algorithm and template matching method are employed to match images and polynomial correction with tiny facet of geometric correction model is employed to correct images. We do experiments using our developed prototype system to correct one scene image of HJ-CCD data. Image matching results of two matching methods above are shown and geometric correction results are shown respectively.

1. INTRODUCTION

Satellite images are material of great interest for many applications such as investigation of environment change, meteorology, etc. In order to use the satellite images in many applications, geometrical correction is required essentially.

Our country is one of the most suffering natural disasters in the world, and one of the most losing due to natural disasters, too. So, HuanJing (HJ)-satellite had been developed to meeting to the requirement of environment monitoring. Since HJ-satellite has been sent successfully in September 6, 2008, in China, productions of precise geometric correction are imminently needed. Moreover, the demand for rapid processing of remote sensing data for disaster is increasing. It is to say that the efficient of geometric correction is more important. So, automatic precise geometric correction for HJ-satellite imagery is an important and urgent task. How to advance the efficiency of geometric correction and how to simplify the geometric correction? Following the development of ICP database system, we will be able to effectively use these data for the purposes like an automated geometric correction for satellite images (because we have to handle so many images, automatic system is indispensable). In the view of the mentioned above, in this paper, we design an automatic precise geometric correction technology flow for HJ-CCD imagery based on image control point database. The whole process mainly contains three technologies: ICP database construction, automatic image matching and model computation.

First of all, it's necessary to introduce HJ-CCD imagery. HJ-A(optical satellite), HJ-B(optical satellite), HJ-C(Radar satellite) satellites constitute HJ-satellite constellation, named "2+1" constellation. HJ-A and HJ-B have been sent successfully in

September 6, 2008, in china. Both of them are installed CCD satellite. The spatial resolution of HJ-CCD imagery is 30 meter, and the radiate resolution is just about 10 bit. Actually, some of the images of the radiate resolution are just 5 bit, which will increase the difficulty of image matching.

Image matching is to match an image with other image that may has different properties. Many strategies, methodologies and algorithms for image matching were presented. Zitova et al. presents a survey of recent image registration techniques covering different application areas. In general, image matching methods are classified into two kinds, one is area-based and the other is feature-based. Area-based methods are more simple than feature-based methods. CC—cross-correlation, MI—mutual information, etc. are all area-based methods. They have two principal limitations: reference and sensed images must have somehow 'similar' intensity functions, either identical (and then correlation-like methods can be used) or at least statistically dependent (this typically occurs in multimodal registration). While Feature-based methods allow to register images of completely different nature (like aerial photograph and map) and can handle complex between-image distortions, such as SIFT algorithm, relax method. spatial relation-based, etc.

Geometric correction model contains rigorous model, such as satellite orbital model, and general model, such as rational function model, polynomial model, affine model, etc. In this paper, the orbital parameters of HJ-satellite were unknown. The mathematical model used to compensate the distortion correction is only general models. It neglects all the sources of distortions but deal with the present ones with the help of control points. This also makes the correction procedure easier in the circumstance of insufficient parameters.

* Corresponding author. tianye.zx@163.com

In section 2, we will represent the principle of precise geometric correction. Technology and algorithm of precise geometric correction will be represented in section 3, which contains automatic image matching technology, two imagery matching algorithms (SIFT and template matching methods), and polynomial correction with tiny facet algorithm. Section 4 will show experimental results. And some conclusions will be drawn in section 5.

2. PRINCIPLE OF PRECISE GEOMETRIC CORRECTION

Figure 1 shows the principle of automatic precise geometric correction for HJ-CCD imagery. From figure 1, we can see that our automatic precise geometric correction for HJ-CCD imagery contains seven parts, details are as follows:

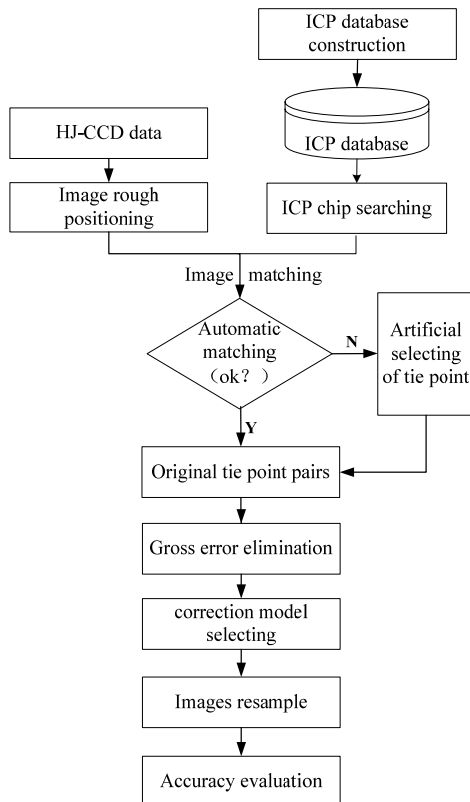


Figure 1. Principle of automatic precise geometric correction for HJ-CCD imagery

- Carrying rough position for original image. Make use of the information of original image's header file to carry rough position.
- ICP database construction. This part will be described in 3.1.
- Tie point pairs matching. Although we achieve automatic image matching, we still offer a way to manually select tie points that we can select tie points manually when automatic image matching failed to select tie points between two special images.
- Gross errors elimination.
- Correction model computation.
- Image resampling.
- Accuracy evaluation.

3. TECHNOLOGY AND ALGORITHM

3.1 Automatic image matching technology based on ICP database

We introduce the ICP database into image matching which can realize the automatic matching of the images. It can simplify the process of traditional tie points selection and advance the efficiency, which used to manual selection.

Figure 2 shows the flow of searching ICP chips from ICP database. First of all, we should construct the ICP database where enough needed ICP chips existed. Second, put original image information as original searching conditions, such as chip ID, getting date, type of sensor, spatial resolution of images, etc, to search needed chips automatically. Third, use image matching method getting tie point pairs. This technology is a key step of realizing automatic image matching.

The front part of Figure 1 shows the scheme of tie point pairs matching. The process is as follows:

- Do gross matching for original image of HJ-CCD data.
- Do searching ICP chips in the ICP database as the reference images using geocoordinates of the original image.
- Automatic image matching based on ICP database, the algorithm is template matching based on Forstener operator.
- If automatic image matching failed, we will go to manual selecting of tie points.

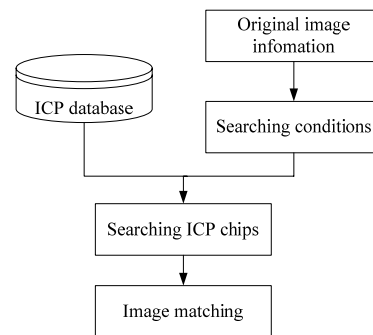


Figure 2. Flow of searching needed ICP chips

3.2 Image matching algorithm

3.2.1 SIFT algorithm: SIFT algorithm is successful in feature matching research areas at present. It transforms image data into scale-invariant coordinates relative to local features. Figure 3 shows the steps of SIFT feature vector generation. The detailed steps of this method are as follows.

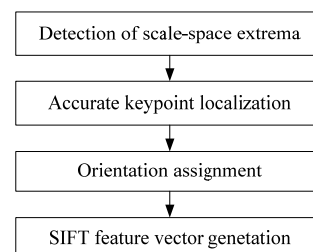


Figure 3. The steps of SIFT feature vector generation

- Extreme value is detected in the different scale of the image, and it is the key-point. Use difference-of-Gaussian function convolved with the image, $D(x, y, \sigma)$, which can be computed

from the difference of two nearby scales separated by a constant multiplicative factor k :

$$D(x, y, \sigma) = (G(x, y, k\sigma) - G(x, y, \sigma)) \times I(x, y)$$

b) The position of key-point is located by the filter of the key-points.

c) The gradient direction of the key-point is determined by the key-point neighborhood. For each image sample, at its scale, the gradient magnitude, $m(x, y)$, and orientation, $\theta(x, y)$, are precomputed using pixel differences:

$$m(x, y) = \sqrt{(L(x+1, y) - L(x-1, y))^2 + (L(x, y+1) - L(x, y-1))^2}$$

$$\theta(x, y) = \tan^{-1} \frac{L(x, y+1) - L(x, y-1)}{L(x+1, y) - L(x-1, y)}$$

d) The feature descriptor is calculated by the feature of the key-point. Then SIFT feature vector will be generated through the above steps.

3.2.2 Template matching algorithm based on Forstner operator: this algorithm contains two phases: Forstner feature point extraction and template matching.

a) Forstner feature point extraction. Firstly, calculate Robert gradient of the pixel. And then calculate the covariance matrix of specified window. Secondly, calculate interesting value q , w .

$$w = \frac{DetN}{trN}$$

$$q = 1 - \frac{(a^2 - b^2)^2}{(a^2 + b^2)^2}$$

Where q is the radian of the pixel of error ellipse,
 w is the power of this pixel.

Finally, use w , q to extract Forstner feature points.

b) Template matching. Calculate correlation coefficient of specified size of window between reference image and original image, and the biggest one connect one pair of tie points.

3.3 Geometric correction model

Geometric correction model mainly classifies two kinds: general geometric correction model and rigorous geometric correction model. General geometric correction contains polynomial, direct linear transformation, affine transformation, rational function model, RPC, etc. In this paper, as previously stated, the orbital parameters were unknown. Under the circumstances, general geometric correction model can be used. Polynomial model is widely used, however, there are a number of factors which bring on images deformation, with a simple polynomial model to approximate the geometric structure deformation of different regions and different sensors will take on some limitations and blindness. Polynomial correction with tiny facet algorithm can solve the problem of images deformation.

In this paper, we adopt polynomial correction with tiny facet algorithm which considers that elevation changes slowly in small areas, and form the control points to Delaunay

triangulation. In a Delaunay triangulation, each triangle is shaped as equilaterally as possible by connecting each ground control point (GCP) to its two nearest neighbors. The elevation can be considered as the same in small areas. We do precise geometric correction using 1st-order polynomial algorithm.

$$x = a_0 + a_1X + a_2Y$$

$$y = b_0 + b_1X + b_2Y$$

Because multiple polynomials are used, local distortion can be corrected. A large number of well-placed GCP's could result in an almost complete correction for any geometrical errors. If the GCP's could be placed with 100 percent accuracy, accuracy would be a function of image resolution and photograph scale.

4. EXPERIMENTS

We develop a prototype system and implement experiments based on this prototype system for HJ-CCD images.

4.1 Image matching results

4.1.1 Image matching results of SIFT algorithm: The original image is an HJ-CCD image with as size of 860,324 KB, and its derived date is September 30th. Chips (reference image) are also HJ-CCD images, and derived date is March 8th.

Figure 4 shows the result of the automatic image matching using SIFT algorithm. We can see that subjective precision meets the requirement. There also exist a few miss matching points.

4.1.2 Image matching results of Template matching algorithm based on Forstner operator: original image is an HJ-CCD image with as size of 943,398 KB, and its derived date of month is July. Chips (reference image) are TM multispectral images, and derived date is November. The image spatial resolution is 30 meters.

Figure 5 shows the result of the automatic image matching using Template matching algorithm based on Forstner operator algorithm. We get 41 tie points which distribute equality.

4.2 Geometric correction results

Polynomial correction with tiny facet model of geometric correction was employed to correct the image together with the above tie points which are automatically matched in the previous step. We adopt bilinear interpolation method to resample the HJ-CCD image. Figure 7 shows the result of geometric correction. It shows at the ratio of 1:1. On the left of the picture is HJ-CCD image, and on the right of picture is geo-coded image of TM. We can see that the accuracy can upto one pixel on subjective precision.

We do precise geometric correction using 1st-order polynomial in each Delaunay triangles. So, residuals could not be attained due to there are no redundant observations. We list 2nd-order polynomial residuals to evaluate the accuracy, shown as appendix table. There are 33 control points, 8 check points and this accuracy can meets our requirement.

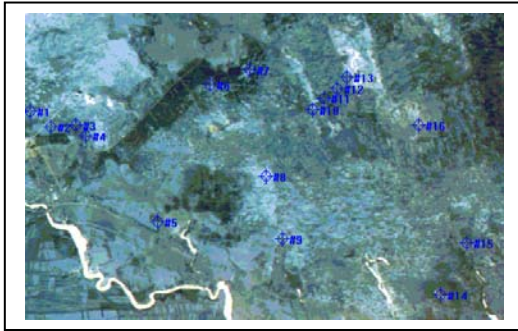


Figure 4. The result of automatic image matching for HJ-CCD imagery using SIFT algorithm

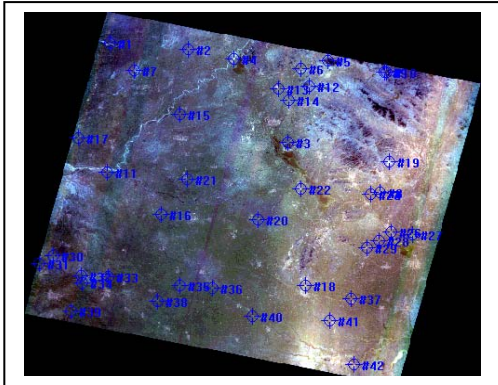


Figure 5. The result of automatic image matching for HJ-CCD imagery using Template matching algorithm based on Forstner operator algorithm

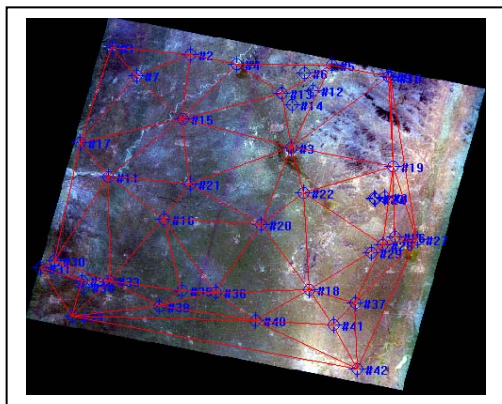


Figure 6. Construction of mesh of Delaunay triangles

5. CONCLUSIONS

An automatic geometric correction technology flow is designed in this paper to automatically correct HJ-CCD images, which has resolution of 30 meters and localized geometric distortion. The technology flow can meet the demand of handling emergencies, due to it simplifies the process of the manual tie points selection and increases the speed of image geometric correction greatly.

As stated previously, geometric correction contains seven parts, they are image rough positioning, ICP database construction, automatic matching of tie point pairs, gross errors elimination, correction model computation, image resample and accuracy evaluation. We introduce the ICP database into geometric

correction which can realize the automatic geometric correction of the images. Template matching method based on Forstner operator algorithm and SIFT algorithm are employed to match the images. And we adopt polynomial correction with tiny facet algorithm model to correct the experiment images. We correct one scene of HJ-CCD image according to our designed technology flow of precise geometric correction. Experiments show that our automatic geometric correction technology is efficient and practical.

We will integrate this technology of automatic precise geometric correction for HJ-CCD imagery into cluster environment, which will reduce the time of image processing greatly.

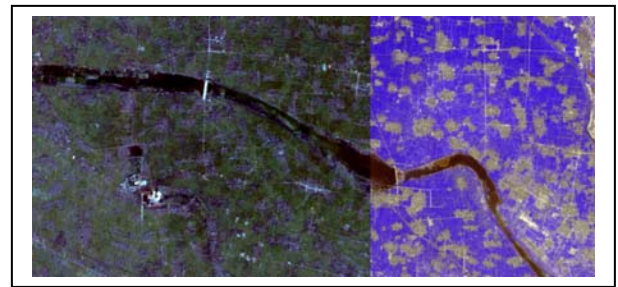


Figure 7. The result of geometric correction

ACKNOWLEDGMENT

This work was supported in part by Chinese Academy of Surveying and Mapping, P.R.China, and in part by National High-Tech Research and Development Program of China under Grant2007AA12Z151, and National Basic Research Program of China under Grant2006CB701303.

REFERENCES

- Xu Jing, "environment and disaster monitor predicting satellite system overview in China," *Satellite Application*, vol.10(1), 2002. pp.25-36.
- Barbar Zitova, Jan Flusser. *Image registration methods: a survey* [J].*Image and Vision Computing* 2003 (21). pp.977-1000.
- Lowe D G, "Distinctive image features from Scale-Invariant keypoints," *International Journal of Computer Vision*, vol. 60(2), 2004, pp. 91-110.
- Brown M, and Lowe D G, "Invariant features from interest point groups," *British Machine Vision Conference*, Shanghai, 2002, pp. 656-665.
- A. Goshtasby, F. Cheng, and B. A. Barksy, "B-splinecurves and surface viewed as digital filters," *Computer Vision, Graphics, and Image Processing*, **52**,1990. pp.264-275.
- Hernâni Gonçalves, José A. Gonçalves, and Luís Corte-Real, "Measures for an Objective Evaluation of the Geometric Correction Process Quality", *IEEE GEOSCIENCE AND REMOTE SENSING LETTERS*, VOL. 6(2), 2009. pp.292-296.
- ZhangJianqing, 2003. *Photogrammetry*, Wuhan University

APPENDIX TABLE. The control points and residuals of 2nd-order polynomial

GCPID	x	y	Residual x	Residual y	RMS	Type
Gcp#1	7620.000	1840.000	1.086	-0.476	1.186	control
Gcp#2	11039.000	1878.000	-2.038	-1.629	2.609	control
Gcp#3	4006.000	2280.000	1.312	0.214	1.329	control
Gcp#4	13094.000	2327.000	-0.170	-0.676	0.697	control
Gcp#5	13171.000	2351.000	-1.223	0.288	1.256	control
Gcp#6	10347.000	2877.000	-0.250	-0.581	0.633	check
Gcp#7	9246.000	2970.000	1.030	2.204	2.433	control
Gcp#8	9601.000	3406.000	2.386	1.179	2.661	check
Gcp#9	5663.000	3955.000	-2.130	0.159	2.136	control
Gcp#10	1973.000	4877.000	-1.959	1.214	2.305	control
Gcp#11	13264.000	5802.000	0.556	2.041	2.116	control
Gcp#12	5931.000	6456.000	-1.548	-1.404	2.090	control
Gcp#13	10034.000	6820.000	2.525	-0.604	2.596	control
Gcp#14	12574.000	7023.000	1.015	-0.620	1.189	check
Gcp#15	12589.000	7029.000	1.003	0.367	1.068	check
Gcp#16	13314.000	8499.000	1.001	-0.780	1.269	control
Gcp#17	14122.000	8608.000	-0.480	-0.502	0.695	control
Gcp#18	12876.000	8824.000	0.184	-0.594	0.622	control
Gcp#19	12460.000	9110.000	-0.595	-0.413	0.724	check
Gcp#20	1060.000	9415.000	-0.156	0.136	0.207	control
Gcp#21	558.000	9707.000	-0.338	0.469	0.578	control
Gcp#22	2050.000	10200.000	1.278	-1.052	1.655	control
Gcp#23	3033.000	10212.000	0.155	0.076	0.173	control
Gcp#24	2100.000	10438.000	-0.580	-0.217	0.619	check
Gcp#25	5635.000	10568.000	-1.422	0.564	1.530	control
Gcp#26	6851.000	10658.000	-0.605	-0.579	0.838	control
Gcp#27	11881.000	11059.000	-0.927	0.606	1.107	control
Gcp#28	4840.000	11171.000	-1.116	-0.144	1.125	control
Gcp#29	1694.000	11553.000	2.022	0.450	2.072	control
Gcp#30	8279.000	11732.000	0.681	0.247	0.724	control
Gcp#31	11100.000	11900.000	-0.874	0.490	1.002	control
Gcp#32	11973.000	13604.000	-0.428	-0.377	0.570	control
Gcp#33	3115.500	1214.500	0.962	-0.181	0.979	control
Gcp#34	5959.500	1468.500	0.255	0.271	0.372	control
Gcp#35	9586.500	5056.500	1.831	0.706	1.962	control
Gcp#36	2998.500	6182.500	-0.107	-2.176	2.179	control
Gcp#37	10039.500	2193.500	1.765	0.219	1.779	check
Gcp#38	12934.500	6977.500	-0.139	0.111	0.178	check
Gcp#39	4984.101	7808.637	-0.748	1.148	1.370	control
Gcp#40	10233.551	10539.436	1.712	0.317	1.741	control
Gcp#41	8502.740	8025.481	-0.323	-0.425	0.534	control